Electronic Supplementary Material (ESI) for Nanoscale.


# Supporting information: Utilising buckling modes for the determination of the anisotropic mechanical properties of $As_2S_3$ nanosheets

**Ming Dong[1], Yiwei Sun[2], David J. Dunstan[1], Dimitrios G. Papageorgiou[2]***

*[1] School of Physical and Chemical Sciences, Queen Mary University of London, London E1 4NS, United Kingdom*
*[2] School of Engineering and Materials Science, Queen Mary University of London, London E1 4NS, United Kingdom*
*Corresponding author's email: d.papageorgiou@qmul.ac.uk*

## 1. Compression induced wrinkles

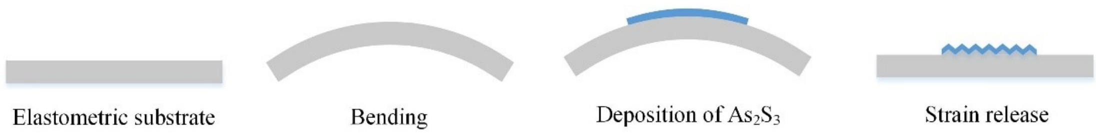


Figure S1. Fabrication of wrinkled $As_2S_3$ flakes. The wrinkles are formed after releasing the pre-bended elastic substrate.

## 2. Polarization-resolved transmission spectroscopy

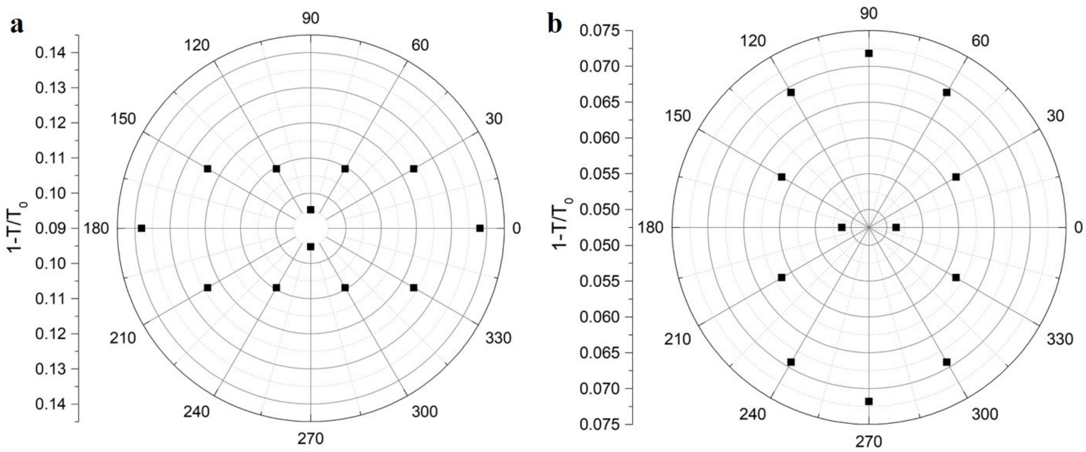


Figure S2. Angular-dependent optical transmission ($T/T_0$) of $As_2S_3$ flakes with wrinkles perpendicular to the (a) AC and (b) ZZ directions as shown in Figure 2. $T$ is normalized to the transmission of the substrate, $T_0$. The angle is defined as the angle between the linear polarizer and the horizontal directions in Fig. 2a and Fig.2b respectively. The transmission is plotted radially according to the axes shown on the left of each plot.

## 3. Elastic modulus for wrinkling

A thin plate under in-plane compression and supported by a soft elastic substrate to which it adheres fails by Euler buckling into a sinusoidal wrinkling. The theory for an isotropic plate is fully worked out[1], but is given in terms of engineering moduli such as Young's modulus and the plane-strain modulus. For a 2D material such as graphene, it can also be convenient to express the theory in terms of 2D elastic moduli. Extending the theory to a general anisotropic plate using these quantities can be very confusing, and so we explain the analysis here from first principles.

### 3.1 Notation and elementary relationships

Stress, strain and the relationships between them, the elastic stiffness constants, are tensors, **σ**, **ε**, and **c**, both in 3D and in 2D. For convenience, we use Voigt notation in which in 3D, second-rank tensor elements with two subscripts *ij*, with *i, j* = 1-3 or *x*, *y*, *z*, are written with one subscript *I* = 1-6 for *xx*, *yy*, *zz*, *yz*, *zx*, *xy*, and similarly four subscripts *ijkl* are condensed to *IJ*). We note that there are no shear stresses in the problems addressed here, so we need only the Voigt subscripts ranging over 1-3. The full description of the infinitesimal (linear) elasticity of an isotropic material is illustrated by finding Young's modulus where we have only a longitudinal (*x*-direction) stress, a longitudinal strain and two perpendicular strains due to Poisson's ratio:

$$\begin{pmatrix} \sigma \\ 0 \\ 0 \end{pmatrix} = \begin{pmatrix} c_{11} & c_{12} & c_{12} \\ c_{12} & c_{11} & c_{12} \\ c_{12} & c_{12} & c_{11} \end{pmatrix} \begin{pmatrix} \varepsilon \\ \varepsilon_{\perp} \\ \varepsilon_{\perp} \end{pmatrix} \tag{S1}$$

Taking the third line, we have

$$0 = c_{12}\varepsilon + (c_{11} + c_{12})\varepsilon_{\perp} \tag{S2}$$

from which the Poisson's ratio is

$$\nu = -\frac{\varepsilon_{\perp}}{\varepsilon} = \frac{c_{12}}{c_{11} + c_{12}} \tag{S3}$$

From the first line of Eq. S1 and using Eq. S3, we have

$$\sigma = c_{11}\varepsilon + 2c_{12}\varepsilon_{\perp} = \left( c_{11} - \frac{2c_{12}^2}{c_{11} + c_{12}} \right)\varepsilon \tag{S4}$$

and the quantity in brackets can be recognised as the Young's modulus *E*.
These expressions can be inverted, so that if we have *E* and ν, we may obtain $c_{11}$ and $c_{12}$ as

$$c_{11} = \frac{1 - \nu}{1 - \nu - 2\nu^2}E \quad and \quad c_{12} = \frac{-\nu}{1 - \nu - 2\nu^2}E \tag{S5}$$

The linear elastic properties of the isotropic material are fully described by the two parameters $c_{11}$ and $c_{12}$, or by *E* and ν. Equally, if we set up the situations in which stress and strain are related by the bulk modulus *B*, the plane-strain modulus $\bar{E}$, or the shear modulus $G = c_{44}$, or any other moduli, we can find how these are related to $c_{11}$ and $c_{12}$. We can recover the well-known relationships between these quantities such as $G = ½E/(1 + \nu)$, which may also be written as $G = c_{44} = ½(c_{11} - c_{12})$.

### 3.2 Anisotropic elasticity

Crystals have lower symmetry than isotropic or spherical and require more constants to define their elasticity. In cubic symmetry, $c_{11}$, $c_{12}$ and $c_{44}$ are independent constants; the relationship given in the previous section for $G$, $E$ and ν does not apply, and the anisotropy may be quantified by the constant $C = 2c_{44} - c_{11} + c_{12}$. In orthorhombic symmetry, as we have here, and in the absence of shear strains, we require the six elastic constants $c_{11}$, $c_{22}$, $c_{33}$, $c_{12}$, $c_{13}$ and $c_{23}$ (or, equivalently, three Young's moduli and three Poisson's ratios or other combinations of six engineering constants).

Note that rewriting Eq.S1 with these six elastic constants and obtaining Young's modulus for a strain $\boldsymbol{\sigma} = (\sigma_1, 0, 0)$ now requires solving the second and third lines simultaneously for the two Poisson's ratios $\nu_{12}$ and $\nu_{13}$ that give rise to $\varepsilon_2$ and $\varepsilon_3$. They are not simple, but they are of the same form and related by interchange of subscripts 2 and 3, and so we display only one of them,

$$\nu_{12} = -\frac{c_{33}c_{12} - c_{23}c_{13}}{c_{22}c_{33} - c_{23}^2} \tag{S6}$$

Young's modulus for strain in the $x$ direction is then $Y_x = c_{11} - c_{12}\nu_{12} - c_{13}\nu_{13}$. It is clearly no simple matter to obtain one of the engineering moduli from known values of six others.

### 3.3 Plane stress and plane strain

Engineering problems often simplify to so-called plane-stress problems or plane-strain problems, and it is therefore common to encounter plane-stress or plane-strain moduli accordingly. The definition of plane stress (strain) is that all stresses (strains) are in the $x$-$y$ plane, and the normal ($z$-direction) stress (strain) is zero. When a 2D material is exfoliated and placed on a substrate, it is rare that it has zero in-plane stress or strain. However, there is zero stress normal to the substrate, so this is a plane stress problem, with

$$\begin{pmatrix}\sigma_1\\ \sigma_2\\ 0\end{pmatrix} = \begin{pmatrix}c_{11} & c_{12} & c_{13}\\ c_{12} & c_{22} & c_{23}\\ c_{13} & c_{23} & c_{33}\end{pmatrix}\begin{pmatrix}\varepsilon_1\\ \varepsilon_2\\ \varepsilon_\perp\end{pmatrix} \tag{S7}$$

On the other hand, when a 2D flake is bent about an axis in the $y$-direction, it is under tension ($\varepsilon_{xx}$) around the outside of the bend, and under compression around the inside. This sets up stresses in the $y$-direction, compressive and tensile respectively, and a shear stress $\varepsilon_{yz}$ within the flake, which tends to cause anticlastic curvature. However, when the flake is much wider than its thickness, these effects can be neglected. The outcome in this case is that the strain in the $y$-direction vanishes, and so this becomes a plane-strain problem, with

$$\begin{pmatrix} \sigma \\ \sigma_y \\ 0 \end{pmatrix} = \begin{pmatrix} c_{11} & c_{12} & c_{13} \\ c_{12} & c_{22} & c_{23} \\ c_{13} & c_{23} & c_{33} \end{pmatrix} \begin{pmatrix} \varepsilon \\ 0 \\ \varepsilon_\perp \end{pmatrix} \tag{S8}$$

from which the bending stiffness may be calculated. The third line gives the relevant plane-strain Poisson's ratio, as

$$\nu_{13} = -\frac{\varepsilon_\perp}{\varepsilon} = \frac{c_{13}}{c_{33}} \tag{S9}$$

and then the first line gives the relevant modulus, by

$$\sigma = c_{11}\varepsilon + c_{13}\varepsilon_\perp = \left( c_{11} - \frac{c_{13}^2}{c_{33}} \right) \varepsilon \tag{S10}$$

The standard solution for the bending stiffness $D$ of an isotropic plate is

$$D = \frac{Eh^3}{12(1 - \nu^2)} \tag{S11}$$

and the quantity $E/(1 - \nu^2) = c_{11} - \frac{c_{12}^2}{c_{11}}$ is often referred to as the plane-strain modulus. So the two plane-strain moduli for the orthorhombic symmetry are quite simple.

### 3.4. Anisotropic materials in 2D elasticity theory

As the archetypical 2D material, monolayer graphene has its carbon nuclei in a single ($x$-$y$) plane. Since the thickness $a_{33}$, the strain $\varepsilon_{33}$ and the modulus $c_{33}$ of a crystal in the $z$-direction are conventionally defined by reference to nuclear $z$-coordinates, this causes some confusion in considering these quantities in monolayer graphene. In graphite, however, there is little or no interaction between in-plane and out-of-plane deformation, i.e. $c_{13} = c_{23} = 0$, to within experimental and theoretical resolution. So it is convenient to ignore all subscripts 3 in the tensor elasticity theory. In considering a monolayer, to attribute to it the quantities that it has in graphite in GPa, divided by the layer spacing in graphite, e.g. $c_{11}^{2D} = c_{11}a_{33}$ in units of $Nm^{-1}$, and $\sigma_1$ likewise, while $\varepsilon_1$ is unchanged – and then to refrain from mentioning the thickness in any analysis. This makes the bending stiffness of monolayer graphene independent of $c_{ij}$, which is correct. It is, however, an approach which does not work so directly for other 2D materials such as monolayer $MoS_2$ or $As_2S_3$, both because they do have nuclei out-of-plane, and because they do have non-zero $c_{13}$ and $c_{23}$. It would be incorrect to take the separation between the nuclei above and below the centre plane as the thickness – as incorrect as taking zero for the thickness of monolayer graphene – and it would be incorrect to take the changes in the separations of these nuclei as defining $\varepsilon_z$. The extension of the electron wave-functions beyond these nuclei must be considered, just as the extension of the π-orbitals of graphene must be considered.

However, the central point here is that 2D elasticity theory can be used, if it would be useful, but only with careful definitions. Consider the plane-strain measurement of a 2D specimen under 3D plane-stress conditions, i.e. $\sigma_z = \varepsilon_y = 0$. In 2D elasticity, we have (with $\boldsymbol{\sigma}$ and **c** components all understood as 2D quantities measured in $Nm^{-1}$)

$$\begin{pmatrix}\sigma_1\\ \sigma_2\end{pmatrix} = \begin{pmatrix}c_{11} & c_{12}\\ c_{12} & c_{22}\end{pmatrix}\begin{pmatrix}\varepsilon_1\\ 0\end{pmatrix} \qquad \text{(S12)}$$

Solving, $\sigma_1 = c_{11}\varepsilon_{11}$. This is *not* the 3D equation divided by $a_{33}$ (compare Eq. S10 above).

Thus our experiments described in the main text that use or determine the 3D plane-strain modulus $\bar{E}_{13}$ determine equally directly the 2D $c_{11}$. We use the notation assignment for directions which is consistent in general 2D materials research and especially for graphene, that is 1 and 2 in-plane, and 3 out-of-plane. We report values of elastic constants with the notation consistent with the majority of 2D materials studies. However, often 2 is used for out-of-plane direction in the $As_2S_3$ literature and attention must be paid to correct conversions of subscripts before comparisons of values are made.

### 3.5. Application to loading by bending a compliant substrate

In these experiments, the substrate is a wide and thick polymer beam which is bent to put the surface in uniaxial tension before the exfoliated flake is deposited. The beam is then relaxed so that the flake is put under uniaxial compression. The energy that is released when wrinkles form or buckling delamination occurs comes from the increase in length of the flake, and goes into the bending of the beam and the deformation of the substrate underneath. For wrinkles that are long compared with their wavelength, none of these deformations cause any displacement of material parallel to the wrinkles, so the strain in this direction is zero and it is the 3D plane strain moduli $\bar{E}$ which enter into the problem. The same applies if the flake is deposited on the unstrained substrate which is then bent to put the flake in compression.

### 3.6 Application to loading by deposition on a non-compliant substrate

When a 2D flake is deposited on a hard substrate such as silicon, it is usually found to be in a state of non-zero in-plane strain, often sufficient to cause buckling by delamination. Since the strain in the flake parallel to the wrinkles is non-zero, it is worth checking if the plane-strain modulus still applies. Taking Eq. S8 and adding a strain in the *y*-direction, we have,

$$\begin{pmatrix}\sigma_1\\ \sigma_2\\ 0\end{pmatrix} = \begin{pmatrix}c_{11} & c_{12} & c_{13}\\ c_{12} & c_{22} & c_{23}\\ c_{13} & c_{23} & c_{33}\end{pmatrix}\begin{pmatrix}\varepsilon_1\\ \varepsilon_2\\ \varepsilon_3\end{pmatrix} \qquad \text{(S13)}$$

and solving these three equations, we obtain,

$$\sigma_1 = \left(c_{11} - \frac{c_{13}^2}{c_{33}}\right)\varepsilon_1 + \left(c_{12} - \frac{c_{13}c_{23}}{c_{33}}\right)\varepsilon_2 \tag{S14}$$

From this, we see that $d\sigma_1/d\varepsilon_1$ is again the plane-strain modulus.

### 3.7 Loading by uniaxial compression of a compliant substrate

For completeness, we note an exception to the general applicability of the plane-strain modulus. That is the experiment of Vella *et al.*[2] in which a film is deposited on an unstrained compliant substrate which is then compressed uniaxially to develop delamination buckling with wrinkles running perpendicular to the compression axis. It is not entirely clear whether this is uniaxial stress or uniaxial strain.[2] Uniaxial stress results in a transverse strain in the substrate, and the extent to which this appears in the film will depend on the relative widths and thickness of the film and the substrate and of the buckling wavelength. Full solutions for different conditions should be checked by the methods above.

## 4. Thickness determination of $As_2S_3$ flakes

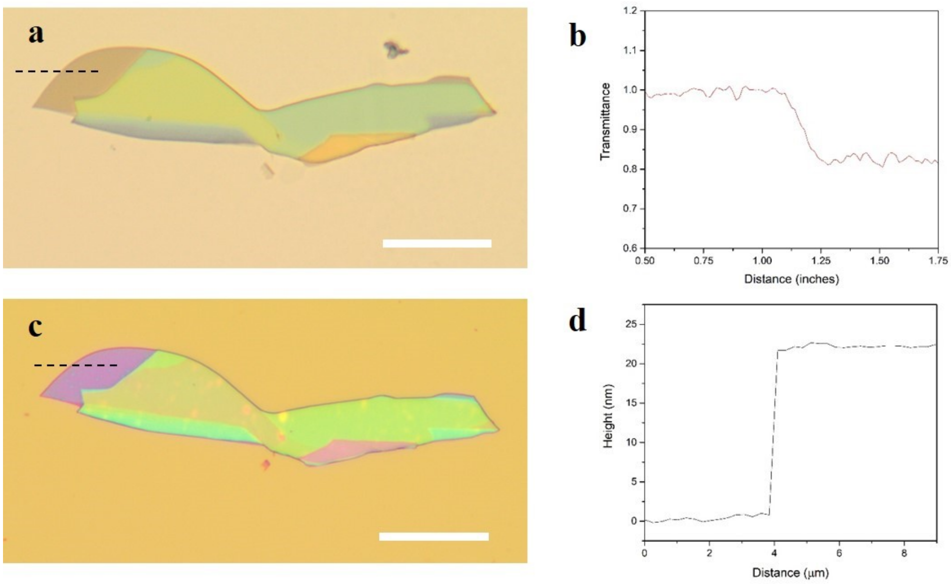


Figure S3. (a) Transmission mode optical image of $As_2S_3$ flake on Gel-film. (b) Optical transmission of the flake along the dashed line in (a). (c) Optical image of the flake transferred to a $SiO_2$/Si substrate. (d) Thickness of the flake measured by AFM along the dashed line in (c). Scale bars, 10 μm.

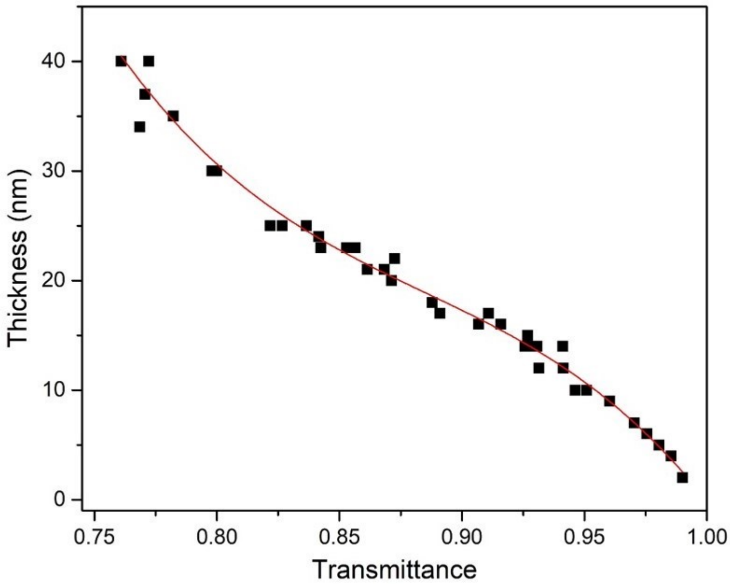


Figure S4. The relationship between thickness and transmittance of $As_2S_3$ flakes. The solid line is the 3rd order polynomial function returned by fitting $a + bx + cx^2 + dx^3$ to the data.

**5. Wavelength determination of $As_2S_3$ wrinkles**

The wavelength of the wrinkles are obtained by the fast Fourier Transform (FFT) of selected regions of the grayscale images using software Gwyddion. The variations of wavelength with thickness for wrinkles perpendicular to the AC and ZZ directions are shown in Figure S5.

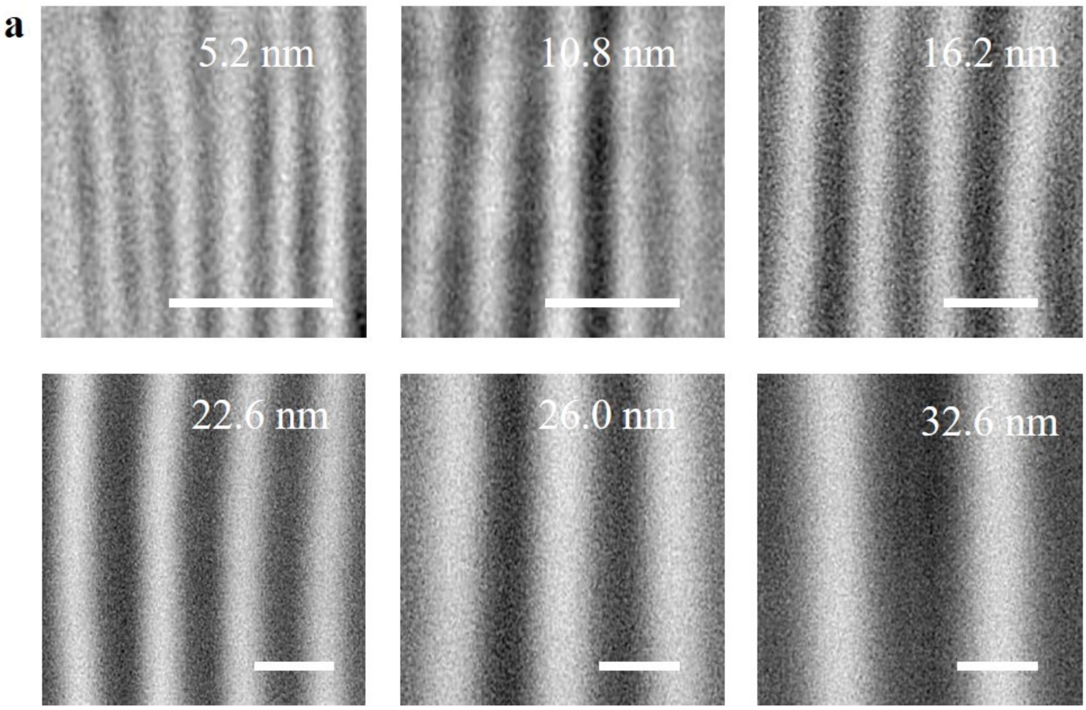

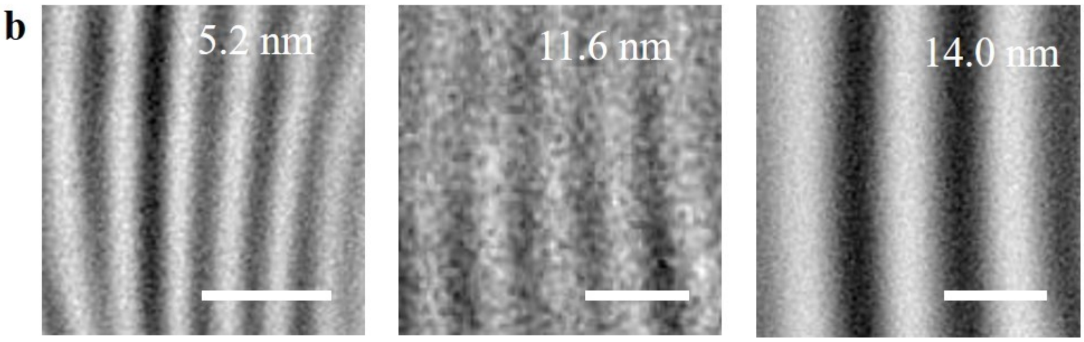


Figure S5. Grayscale optical microscopy images of $As_2S_3$ flakes of different thickness with wrinkles perpendicular to (a) the AC direction and (b) the ZZ direction. Scale bar, 2.5 μm.

## 6. Buckling modes validation

It may be questioned whether the attributions of wrinkling and buckling delamination are correct. However, it is also readily tested by the data we report. For the experiments we identify as delamination, plots of wavelength against thickness (λ-*t*) as in Eq.2 for wrinkling show large scatter (red data-points in Fig. S6). To get a quantity that should be proportional to *t* according to delamination theory (Eq. 2), we construct a corrected wavelength $\lambda'$ by multiplying λ by $t^{1/4}$, by $A^{1/2}$, and by $\Gamma^{1/4}$. Plotting $\lambda'$ against *t*, we see that the scatter collapses onto a straight line (blue data-points in Fig. S6); moreover, fitting with $y = a + bx$, the values of *a* returned are zero within uncertainties, as expected from Eq.2. This is conclusive evidence that this data corresponds to delamination. To quantify this conclusion, we note that the log-likelihoods of the fits[3] show differences in favour of the delamination model of 9.0 (Si), 7.8 (PMMA) and 9.9 (PDMS), which in the context of Bayes theorem correspond to probabilities (odds on) the delamination model of 8050:1 (Si), 2430:1 (PMMA) and 20700:1 (PDMS)[3].

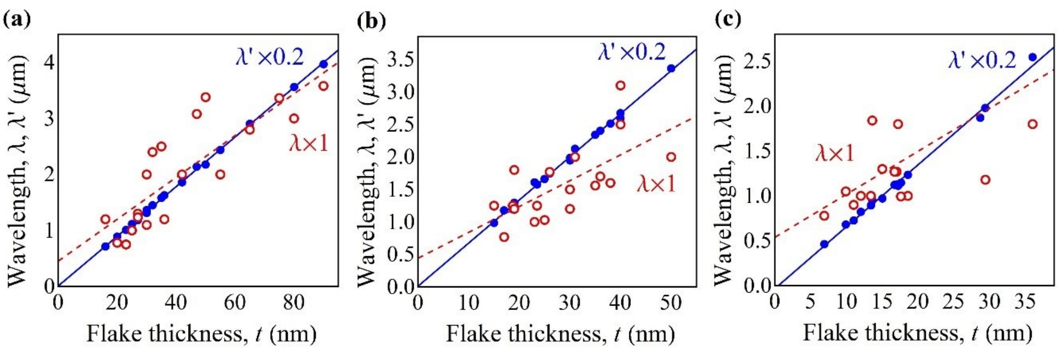


Fig. S6. The data for delamination buckling on (a) silicon, (b) PMMA and (c) PDMS is plotted according to the wrinkling formula, Eq.2, λ against *t* (open red data points) and fitted with $y = a + bx$ (dashed red line). According to the delamination formula, Eq.3, the quantity $\lambda' = \lambda t^{1/4} A^{1/2} \Gamma^{1/4}$ should be proportional to *t* so this is plotted (solid blue data points) and fitted with $y = a + bx$ (solid blue line). The vertical scale is reduced by a factor of five to bring the $\lambda'$ data conveniently onto the $\lambda$-$t$ graph.

To show that delamination did not occur in the wrinkling experiments, the converse argument can be used. They fit well Eq.2 with a zero intercept, and from Fig.S6 this would be a very surprising outcome if delamination was occurring. From Eq.3, it could only happen if $A$ was accurately proportional to $t^{1/2}$ (to give $\lambda \propto t$). Theoretically, $A$ is expected to be proportional to $t^1$ (and to vary with the compressive strain in the flake). It was not convenient to measure $A$ in the wrinkling experiments, but we kept the applied strain constant (0.05 compressive). This would give $\lambda \propto t^{5/4}$, which fits the data very badly, with log-likelihoods at –20 (AC) and –11 (ZZ) against the linear fits of Fig.3. And the actual strain was certainly much less (we estimate 0.05%) and would have varied with the length of each specimen, giving rise to scatter in Fig. 2.

## References


1. A. L. Volynskii, S. Bazhenov, O. V. Lebedeva and N. F. Bakeev, *J. Mater. Sci.*, 2000, **35**, 547-554.
2. D. Vella, J. Bico, A. Boudaoud, B. Roman and P. M. Reis, *Proc. Natl. Acad. Sci. U. S. A.*, 2009, **106**, 10901-10906.
3. D. J. Dunstan, J. Crowne and A. J. Drew, *Scientific Reports*, 2022, **12**, 993.